

### Exotic diffractive dissociation in hadronic collisions

C. E. Navia, C. R. A. Augusto, and F. A. Pinto

*Instituto de Física, Universidade Federal Fluminense, 24210-130, Niterói, Rio de Janeiro, Brazil*

E. H. Shibuya

*Instituto de Física, Universidade Estadual de Campinas, 13081-970, Campinas, Sao Paulo, Brazil*

(Received 9 May 1994)

A full Monte-Carlo simulation of Centauro-like events is carried out using a model where these events are a result of isotropic decaying of “exotic fireballs” coherently produced in diffractive dissociation. The input testaments to the event generator are explained in detail and we find that the model predictions are in agreement with available data from emulsion chamber experiments. Centauro-type events at collider experiments are also reexamined and discussed within this context. We show that, at the extremely high energy region  $E_0 \geq 10^5$  TeV, an exotic dominant channel is consistent with experimental data.

PACS number(s): 96.40.De, 13.85.Tp

#### I. INTRODUCTION

Cosmic-ray experiments have shown strong, experimental evidence of unusual events and processes in the PeV energy region, [1, 4]. Among these events considered as exotic, the most clear and indisputable is Centauro I, reported by the Brazil-Japan Collaboration.

The emulsion chamber detector used by the Brazil-Japan Collaboration at Chacaltaya station (5220 m above sea level) has a two story structure: the upper detector for electromagnetic and hadronic components, produced in the nuclear interaction of cosmic-ray particles with atmospheric nuclei (nitrogen and oxygen), the target layer (carbon) on the upper level, and the lower detector for hadron-carbon interaction (*C* jets) observation on the lower level (see Fig. 1).

A family (hadrons,  $\gamma$ , and  $e^\pm$  with common origin) seen in the upper detector is always several times larger, in number as well as in energy, than its continuations in the lower detector. However, a big surprise was an event

detected in chamber 15, with the contrary situation (see Fig. 1), and it was called a Centauro event.

The suspicion that the event might have happened during a short period of assembling or removing the chamber was eliminated because the upper detector is always mounted before the lower detector and the lower chamber is always the first to be removed.

Another important characteristic was that the production height of  $50 \pm 15$  m estimated from triangulation (divergences between shower position at different depths of the chamber) shows that the Centauro event has a large transverse momentum with a mean around  $\langle P_T \rangle = 1 \sim 2$  GeV/*c* (about 3 times larger than the mean  $P_T$  observed in multiple meson production). The small production height also excludes the possibility of cascade fluctuation that together with the absence of  $\gamma$  rays and, consequently  $\pi^0$ 's, shows that the unbalanced condition of the charge ratio (cf.  $N_{\pi^0}/N_{\pi^\pm}$ ) cannot be attributed to the statistical fluctuation of a normal ratio, because hadrons are too large to allow such a big fluctuation. These facts

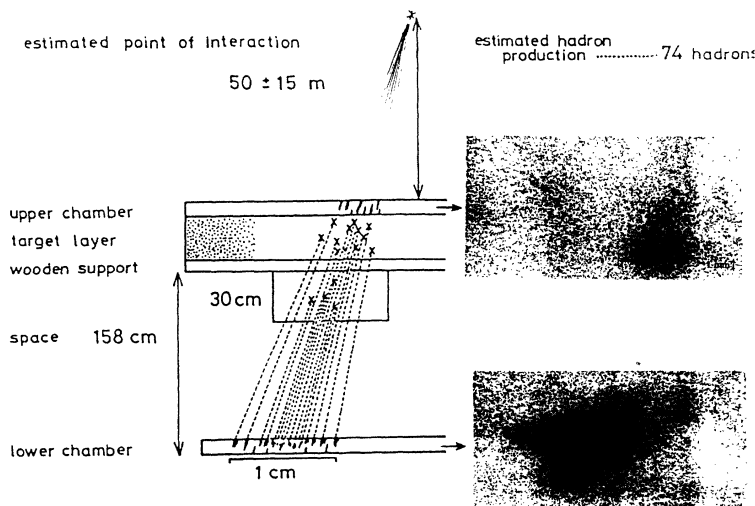


FIG. 1. Schematic view of structure of Chacaltaya two-story chamber, together with photographs of Centauro I as viewed in x-ray films of the upper and lower chambers.

suggest that the produced particles are hadrons heavier than pions, assumed to be baryons (nucleons) as an attempt.

Thus, the first event (Centauro I) was a discovery; a systematic survey was made for events of the same type, and seven events were reported: six from the Chacaltaya chamber and one from the Pamir Chamber [2]. In Table I are listed the main characteristics observed in events such as Centauro, based mainly on the Chacaltaya emulsion chamber. In Table II the experimental values of the maximum pseudorapidity  $\eta_{\max}$ ,  $\langle\eta\rangle$  both in the c.m. system (c.m.s.) frame, and  $\langle P_T^{\gamma}\rangle$  are listed, on the basis of seven Centauro events (atmospheric families), of which the primary energy is normalized to  $E_0 = 1650$  TeV in the laboratory system, corresponding to Fermilab Tevatron energies  $\sqrt{s} = 1.8$  TeV assuming proton incidence.

Using abnormal hadron dominance among its secondaries in families as criteria, events with the same hadron nature of Centauro I were found, the difference being their smaller multiplicity (hadron numbers between 10–20 and they were called mini-Centauro events. In Table III are summarized some details of 15 events such as mini-Centauro events, and in Table IV the experimental values of the maximum pseudorapidity  $\eta_{\max}$ ,  $\langle\eta\rangle$  both in the c.m.s. frame, and  $\langle P_T^{\gamma}\rangle$  on the basis of 15 selected mini-Centauro (atmospheric) interactions of which the primary energy is normalized to  $E_0 = 940$  TeV in the laboratory system, corresponding to  $\sqrt{s} = 1.3$  TeV and 9 events such as mini-Centauro events produced in the target layer of the Chacaltaya chamber of which the incidence energy is normalized to  $E_0 = 100$  TeV in the laboratory system, corresponding to  $\sqrt{s} \sim 430$  GeV are shown, in both cases with the assumption of proton incidence.

On the other hand, a systematic analysis [3, 4] of high energy hadron- $\gamma$  families, not far from the PeV energy region, shows that a global characteristic of cosmic-ray nuclear interactions is different from that from the lower energy region; an extensive comparison among family data and simulation and analytical calculations shows an agreement among them, when exotic channels are in-

cluded in the calculation [5]. However, there is no consensus about it in HEP (high energy physics) and, according to Ref. [6], all these peculiarities can also explained by cascade fluctuations.

In this work we carry out a simulation of Centauro and mini-Centauro events, on the basis of a model where these events are a result of the isotropic decaying of exotic fireballs coherently produced in diffractive dissociation of hadrons (nucleons), as suggested by Goulios [7, 8, 3]. We show that model predictions such as the production energy threshold, midrapidity, mean transverse momentum, and others characteristic to both Centauro and mini-Centauro events, are in agreement with data from emulsion chamber experiments. Centauro species at collider experiment are reexamined and the model predictions for the pseudorapidity distribution for both the CERN Super Proton Synchrotron ( $SppS$ ) and Fermilab are shown and compared with the “normal” diffractive pseudorapidity distribution.

On the other hand, we show that examples of mini-Centauro-like events in nuclear interactions of hadrons with the target layer of the Chacaltaya chamber support the Centauro species being the result of an exotic nuclear interaction between hadrons (ordinary or novel nature hadrons) with nuclei (or nucleons), and also that exotic fireballs have a lifetime short so as to be irrelevant to the analysis.

Finally, we show also that to reproduce the experimental cosmic-ray family flux it is necessary to introduce a dominant exotic channel in the extremely high energy region  $E_0 \geq 10^5$  TeV.

## II. EXOTIC DIFFRACTIVE DISSOCIATION

The few clean events such as Centauro events are strong experimental evidence of exotic interactions, but are not enough to elucidate the whole mechanism of the “so-called” multiple baryon production and only a rude algorithm was developed [3,9], using an exotic diffractive model mounted on the basis of experimental data

TABLE I. Main characteristics of Centauro events.

Event number	I	II	III	IV	V	VI	Pamir
Total hadron observed	49	32	37	38	31	30	22
Total energy (TeV)	221.6	179.0	168.5	143.8	166.7	487.5	444
$N_h$ estimated top chamber	71	66	63	58	45	40	45
$\sum E_h^{(\gamma)}$ (TeV)	321.0	369.2	286.0	219.5	241.9	900	700
$N_{\gamma,e}$ estimated top chamber	1	0	17	51	31	15	55
$\sum E_{\gamma}$ (TeV)	9.0	0.0	66.2	118.6	107.7	95.2	372.5
Height of interaction in meter	50	80	230	500	400	800	700
$N_h$ estimated at interaction	74	71	76	90	63	80	77
$\sum E_h^{(\gamma)}$ (TeV)	330	370	350	340	350	1500	1000
$N_{\gamma,e}$ estimated at interaction	0	0	0	4	0	?	?

TABLE II. Experimental normalized characteristic on the basis of seven events like Centauro where the primary energy is normalized at  $E_0 = 1650$  TeV ( $\sqrt{s} = 1.8$  TeV), assuming proton incidence.

$\langle \eta \rangle$ in c.m.s	$\langle P_t^\gamma \rangle$ (GeV/c)	$\eta_{\max}$
$2.3 \pm 0.3$	$0.35 \pm 0.15$	7.5

and any similarities with “normal” diffractive dissociation and that is described in this work using the DIFFR algorithm reported by UA5 Collaboration [10].

### A. Diffractive mass sampling

It is well known that in “normal” single diffractive dissociation the diffractive mass  $M_X$  expressed as

$$X = M_X^2/s, \quad (1)$$

where  $\sqrt{s}$  is the c.m. energy, has a distribution such as

$$dN/dX = 1/X, \quad (2)$$

with the “coherent” condition  $X < 0.05$  and with a lowest diffractive mass of 1.08 GeV and an upper diffractive mass limit of  $0.224 \sqrt{s}$  (or  $M_X = 122$  GeV at  $\sqrt{s} = 545$  GeV and  $M_X = 403$  GeV at  $\sqrt{s} = 1800$  GeV). Thus, at collider energies the diffractive mass values cover the region of Centauro and especially mini-Centauro fireball masses, estimated as  $\sim 200$  GeV for Centauro and  $\sim 35$  GeV for mini-Centauro events.

The experimental data of the pseudorapidity ( $\eta = -\ln \tan \theta/2$ ) distribution in both Centauro and mini-Centauro events are consistent with a nearly Gaussian distribution expressed in the c.m.s. as

$$\frac{dN}{d\eta} = \frac{N}{2[\cosh(\eta - \langle \eta \rangle)]^2}, \quad (3)$$

centered in  $\langle \eta \rangle$ ; these characteristics strongly support a diffractive formation and the subsequent isotropic decay of an exotic fireball in  $N$  secondaries and the fireball mass can be obtained as

$$M = 4/\pi \sum E_T = 4/\pi (\langle E_T \rangle N), \quad (4)$$

where  $E_T$  is the transverse energy  $E_T = \sqrt{P_T^2 + m^2}$  and  $N$  the multiplicity, using the values listed in Tables II and IV (note that  $P_T^\gamma$  is the part of the  $P_T$  seen as electromagnetic energy, with  $P_T^\gamma \sim k_\gamma P_T$  and  $k_\gamma$  is the “so-called”  $\gamma$ -ray inelasticity estimated to be  $\sim 0.2$ ); we find  $M_C \simeq 200$  GeV for Centauro events, and  $M_{MC} \simeq 35$  GeV for mini-Centauro events.

It is remarkable that the experimental values of  $\langle \eta \rangle$  listed in Tables II and IV are in agreement with the diffractive model predictions to the pseudorapidity of fireballs in the c.m.s frame expressed as  $\langle \eta \rangle = \ln(\sqrt{s}/M)$ .

Experimental data of exotic events are consistent with discrete values for a fireball mass around  $M_C \simeq 200$  GeV for Centauro events and  $M_{MC} \simeq 35$  GeV for mini-Centauro events. However, a Gaussian fluctuation was introduced in the code generator of exotic fireball mass, with  $\langle M_C \rangle = 200$  GeV and a standard deviation  $\sigma = 25$  GeV for the Centauro fireball and  $\langle M_{MC} \rangle = 35$  GeV and  $\sigma = 3.2$  GeV for the mini-Centauro fireball.

TABLE III. Main characteristics of mini-Cenaturo events. Numbers in parentheses concern a shower with  $E_\gamma / \sum e_\gamma = 0.03$ .

Event No.	$\sum E_\gamma$ (TeV)	$N_h$	$N_\gamma$	$\sum E_h^\gamma$ (TeV)	$Q_h$
19-206S-161I <sup>a</sup>	132.1 <sup>a</sup>	7(7)	10(3)	85.6(85.6)	0.72(0.85)
19-139S-105I <sup>a</sup>	114.0	7(7)	2(0)	100.0(100.0)	0.95(1.0)
19-139S-104I <sup>a</sup>	67.1	6(6)	7(7)	39.9(39.9)	0.59(0.59)
21-138S-106I <sup>a</sup>	161.0	9(3)	10(0)	105.8(84.7)	0.70(1.0)
21-133S-90I <sup>a</sup>	112.0	6(6)	5(5)	76.1(76.1)	0.68(0.68)
18-P08S-70I <sup>a</sup>	469.6	16(7)	7(0)	443.5(393.5)	0.94(1.0)
18-20S-100I	87.4	9(9)	4(1)	69.4(69.4)	0.88(0.95)
18-170S-138I	437.1	12(9)	14(0)	350.1(329.0)	0.83(1.0)
18-155S-126I	188.0	10(6)	18(2)	92.0(82.0)	0.57(0.82)
18-179S-130I	161.2	9(6)	17(6)	75.8(66.6)	0.51(0.61)
18-99S-78I	78.2	9(8)	4(4)	52.6(49.6)	0.73(0.72)
18-2S-3I	210.0	7(5)	16(1)	140.0(128.0)	0.67(0.93)
18-57S-35I	507.6	7(5)	4(0)	482.3(462.3)	0.95(1.0)
17-89S-42I	58.8	7(7)	2(2)	50.1(50.1)	0.90(0.90)
17-31I	96.6	16(8)	0(0)	(62.8)	1.0(1.0)

<sup>a</sup>Events with altitude of interaction determined: 19 – 139S – 105IH =  $330 \pm 50$  m, 19 – 206S – 161IH =  $300 \pm 100$  m.

TABLE IV. Experimental normalized characteristic of mini-Centauro-like events, assuming proton incidence.

Number of events	Normalized energy $\sqrt{s}$ (GeV)	$\langle\eta\rangle$ in c.m.s	$\langle P_t^{\gamma}\rangle$ (GeV/c)	$\eta_{\max}$
15	1300	$3.8 \pm 0.3$	$0.35 \pm 0.15$	7.22
9	430	$2.7 \pm 0.3$	$0.35 \pm 0.3$	6.1

### B. Cross section for exotic diffractive dissociation

Perhaps the threshold energy and the energetic dependence of the cross section for the exotic event production are the most delicate points to be treated.

Even if the trigger used at collider experiments is sensitive essentially to nondiffractive events, the negative results of experimental search for Centauro events at  $Spp\bar{S}$  (CERN), [11] suggest a threshold energy for a Centauro species near to  $\sqrt{s} \sim 540$  GeV. This threshold value is consistent with other values obtained under the theoretical assumption; for instance, the diffractive production of an exotic fireball requires the condition [8]

$$M_X^2/s \leq 0.01, \quad (5)$$

and using the values of Tables II and IV we find  $(\sqrt{s})_{\text{th}} \sim 2000 \pm 500$  GeV for Centauro events  $(\sqrt{s})_{\text{th}} \sim 350 \pm 120$  GeV for mini-Centauro events.

A similar threshold value for mini-Centauro events is predicted by the threshold model [12], and that introduced the threshold forward elastic amplitude  $A = A_0 + A_{\text{th}}$  necessary to make good fits in both  $\rho = \frac{\text{Re}A}{\text{Im}A}$  and  $\sigma_{\text{tot}} = \frac{4\pi}{k} \text{Im}A$ , the threshold energy to  $A_{\text{th}}$  is around  $\sqrt{s} \sim 520$  GeV and needs a new particle of mass  $\sim 30$  GeV (consistent with the mini-Centauro fireball mass) called  $\eta_6$  (color-sextet quark  $\eta$ ) with two types of decay: as  $\eta_6 \rightarrow 2\gamma$  decay like ‘‘geminion’’;  $\eta_6 \rightarrow \text{hadrons}$  decay like a mini-Centauro fireball.

It is well known that the single diffractive cross section is proportional to  $1/M_X^2$ . Thus, the ratio of the cross section of Centauro and mini-Centauro event production can be estimated as

$$\frac{\sigma_C}{\sigma_{\text{MC}}} = \frac{M_{\text{MC}}^2}{M_C^2} \sim 0.03. \quad (6)$$

In order to examine down to what energies the Centauro-like events could be detected, a search for the Centauro species has been carried out in  $C$  jets (a nuclear collision produced in a target layer of the Chacaltaya chamber) by the Chacaltaya Collaboration, and shows that unusual  $C$  jets occur with non-negligible frequency, until the energy region is around 100 TeV or  $\sqrt{s} = 447$  GeV in the c.m. frame. This value is consistent with the exotic diffractive model prediction.

On the other hand, emulsion chamber experiments at mountain altitudes have observed that the ‘‘ $\gamma$ -ray’’ family flux [4] is much lower than the simulated results based in the so-called ‘‘ln  $s$ ’’ extrapolations of models (that reproduce the accelerator data in the lower energy region) and using the so-called ‘‘normal’’ chemical primary composition.

These discrepancies can be reduced using so-called Fe-dominance composition in the primary cosmic-ray flux. However, recent results of the direct observation on primary cosmic-ray composition, reported by the JACEE Group [13], as well as Ref. [14], have shown there is no indication that the chemical composition is changed rapidly in the energy region around  $\sim 10^{15}$  eV. Another alternative is the inclusion of exotic processes in nuclear collision.

We show in Sec. VI that assuming the following assumptions it is possible to reproduce the experimental data for the electromagnetic family flux. (1) The total inelastic cross section is related as

$$\sigma_{\text{ine}} = \sigma_{\text{normal}} + \sigma_{\text{exotic}} \quad (7)$$

with

$$\sigma_{\text{normal}} = \sigma_{\text{ND}} + \sigma_{\text{DD}} + \sigma_{\text{SD}} \simeq \sigma_{\text{ND}} + \sigma_{\text{SD}}, \quad (8)$$

where  $\sigma_{\text{ND}}$ ,  $\sigma_{\text{DD}}$ ,  $\sigma_{\text{SD}}$ , and  $\sigma_{\text{exotic}}$  are the cross sections for nondiffractive, double diffractive, single diffractive, and exotic diffractive processes, respectively. (2) A Hillas’s parametrization [15] to the energy dependence of the inelastic cross section is written as

$$\sigma_{\text{ine}} = \sigma_0 [1 + 0.0273 \epsilon + 0.01 \epsilon^2 \theta(\epsilon)] \text{ mb} \quad (9)$$

with  $\epsilon = \ln(E/200 \text{ GeV})$  with  $E$  in laboratory system and  $\sigma_0 = 32.2$  for nucleon-nucleon collisions,  $\sigma_0 = 20.3$  for  $\pi$ -nucleon collisions, and  $\theta(\epsilon)$  is the step function, summarized in Fig. 2 and assuming the ratio between the single diffractive cross section and nonsingle diffractive as

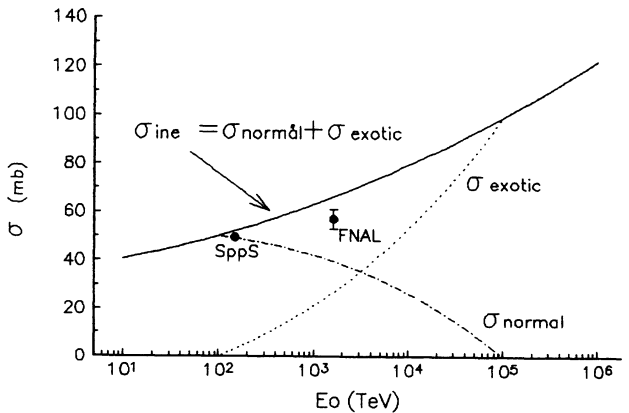


FIG. 2. Energy dependence of inelastic cross section in  $pp$  collisions, according to Hillas’s parametrization, plotted as the sum of inelastic cross sections of ‘‘normal’’ interactions and exotic interactions.

$\sigma_{sd}/\sigma_{ine} = 0.19$  agrees with experimental data (see Fig. 3).

(3) The branching ratio of the “exotic diffractive channel” (Centauro and mini-Centauro events) increases with incident baryon energy as

$$P_{exotic} = 0.333 \ln(E_N/100 \text{ TeV}). \quad (10)$$

Thus, according to the prediction of this model, around 6% of diffractive events at  $\sqrt{s} = 545$  GeV are mini-Centauro-like events and at  $\sqrt{s} = 1.8$  TeV (Fermilab Tevatron) around 1.5% of diffractive events are Centauro-like events and around 60% of diffractive events are mini-Centauro-like events.

### C. Four-momentum transfer and transverse momentum

In “normal” diffractive dissociation, the minimum four-momentum transfer required for the excitation of a nucleon (with mass  $m_p$ ) to a mass  $M_X$  is

$$|t_{\min}|^{1/2} \sim m_p M_X^2/s; \quad (11)$$

we used this condition also for exotic diffractive dissociation, because relation (11) was obtained using only kinematical considerations. Thus, according to the DIFFR algorithm the emission angle of an excited cluster (fireball) is generated through an exponential distribution for the four-momentum transfer as

$$dN/d(-t) \rightarrow \exp(-B t) \text{ with } B = 0.7. \quad (12)$$

From thermodynamics considerations, the transverse momenta ( $P_T$ ) of secondary hadrons emitted from isotropic decay of an exotic fireball (in its own referential system) are obtained using an exponential law, together with the assumption that the exotic fireball is emitted with a four-momentum  $(-t)$  in the c.m.s. obtained with a distribution described above.

### D. Multiplicity

In “normal” diffractive events, the majority of secondary particles emitted when the clusters decay are pi-

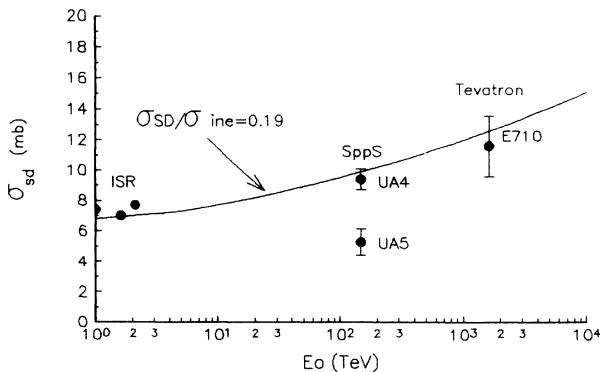


FIG. 3. Energy dependence of single diffractive cross sections in  $p\bar{p}$  collisions, expressed as 19% of the inelastic cross section.

ons and the code generators for the number of charged particles employed by the DIFFR algorithm are NBD (negative binomial distribution) for  $k > 0$ , and Poisson distribution for  $k < 0$ , with  $1/k = -0.104 + 0.024 \ln(M_X^2)$ .

On the other hand, for exotic diffractive events the secondary charged particles are assumed as only nucleons and antinucleons (without pions) and the multiplicity is generated using a Poisson distribution with  $\langle N \rangle = 100$  for Centauro and  $\langle N \rangle = 15$  for mini-Centauro events.

It is remarkable that exotic fireball decay is closed only with isotropic decay. However, to reproduce experimental data of “normal” diffractive events it is necessary to introduce cylindrical decay for events with a high mean transverse momentum ( $\langle P_T \rangle > 0.5$  GeV/c) [10]; thus, the cluster decay can be as isotropic for  $\langle P_T \rangle < P_{\text{cut}}$ , and cylindrical for  $\langle P_T \rangle > P_{\text{cut}}$ , with  $P_{\text{cut}} = 0.5$  GeV/c.

### III. COMPARISON WITH EMULSION CHAMBER DATA

The predictions of exotic diffractive dissociation of the pseudorapidity distribution for Centauro events at  $\sqrt{s} = 1.8$  TeV are shown in Fig. 4 and also compared with experimental data, on the basis of seven Centauro events, normalized at  $\sqrt{s} = 1.8$  TeV. In Figs. 5 and 6, predictions of exotic diffractive dissociation of the pseudorapidity distribution for mini-Centauro events are shown and compared with experimental data in two different energy ranges  $\sqrt{s} = 1300$  and 430 GeV, respectively. For all cases the kinematics of nucleon-nucleon collisions were used in the normalization.

Figure 7 shows the prediction of the exotic diffractive model to the energy-weighted lateral spread of secondary hadrons under the Centauro hypothesis, computed as  $E_h^2 R_h = HK_\gamma P_T$ , where  $P_T$  is obtained from Monte Carlo methods,  $H$  is the interaction height above the chamber ( $H \sim 50$  m for Centauro I), and  $K_\gamma$  is the “ $\gamma$ -ray” inelasticity; the results for three different values of

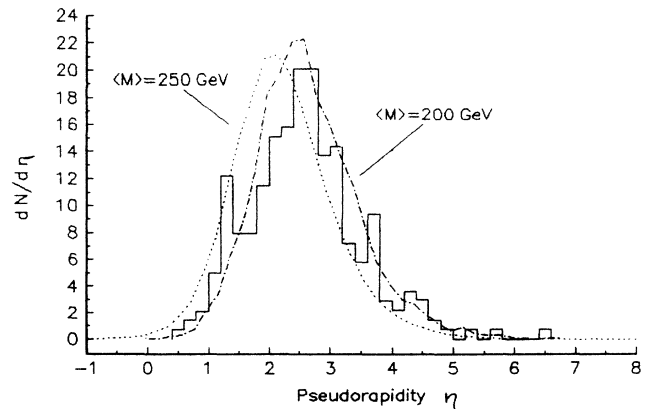


FIG. 4. Pseudorapidity distribution, histograms represent Chacaltaya experimental data on the basis of seven (superimposed) atmospheric Centauro events, normalized at  $\sqrt{s} = 1.8$  TeV and assuming proton incidence. The dashed and dotted lines are obtained from simulation calculation, using the exotic diffractive model for Centauro production.

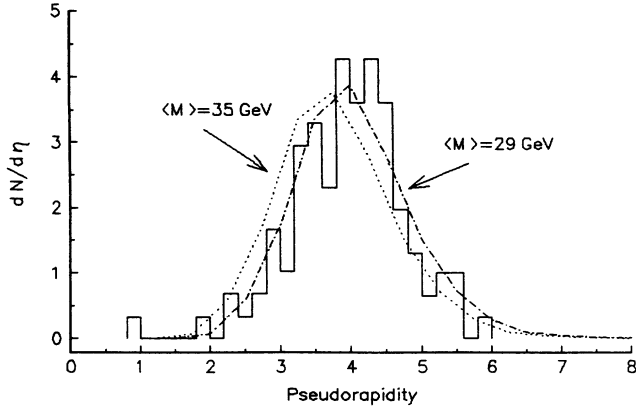


FIG. 5. The same as Fig. 4, where histograms represent Chacaltaya experimental data, on the basis of 15 (superimposed) atmospheric mini-Centauro events, normalized at  $\sqrt{s} = 1.3$  TeV and assuming proton incidence. The dashed and dotted lines are obtained from simulation calculation, using the exotic diffractive model for mini-Centauro event production.

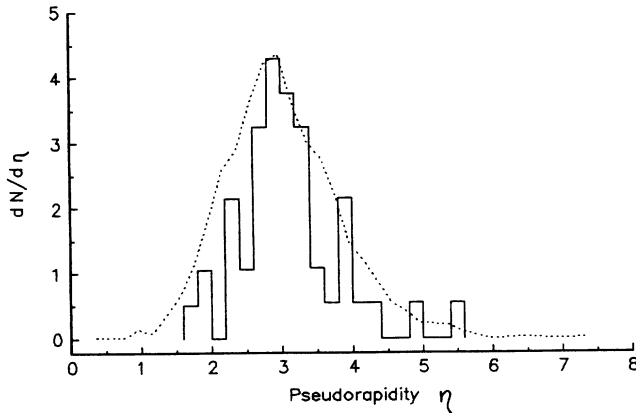


FIG. 6. The same as Fig. 5, where experimental data are plotted on the basis of nine (superimposed) mini-Centauro events produced in the target layer of the Chacaltaya chamber  $C$  jets, normalized at  $\sqrt{s} = 447$  GeV and assuming proton incidence.

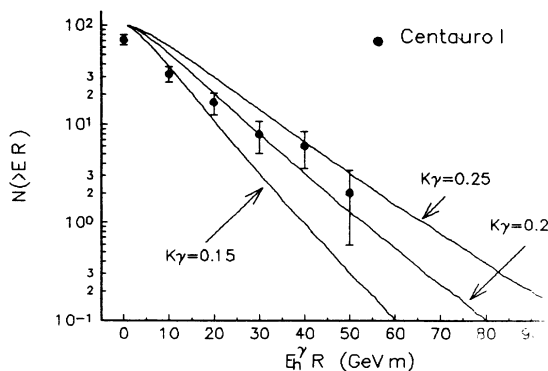


FIG. 7. Prediction of exotic diffractive model to the energy-weighted lateral spread of secondary hadrons under Centauro hypothesis, computed as  $E_h^\gamma R_h = H K_\gamma P_T$ , where  $P_T$  is obtained from the Monte Carlo method,  $H$  is the interaction height above the chamber ( $H \sim 50$  m for Centauro I), and  $K_\gamma$  is the “ $\gamma$ -ray” inelasticity; the results for three different values of  $K_\gamma$  are compared with experimental data of Centauro I events.

$K_\gamma$  are compared with the experimental data of Centauro I events.

#### IV. CENTAURO-LIKE EVENTS AT COLLIDER EXPERIMENTS

The possible observation of Centauro-like events at  $Spp\bar{S}$  ( $\sqrt{s} = 540 - 900$  GeV) has been investigated, with negative results [10,11]. Several arguments answer this result by claiming that the expected production threshold energy for Centauro events [ $(\sqrt{s})_{th} \sim 2000 \pm 500$ ] is larger than the energy used at the  $Spp\bar{S}$  collider experiment; however, the threshold energy for mini-Centauro events [ $(\sqrt{s})_{th} \sim 350 \pm 120$  GeV] is close to the main energy used at  $Spp\bar{S}$  experiments; thus the mini-Centauro channel must have a very small signal. Second, the search for the Centauro phenomenon reported by the UA5 Group is made on the basis of modifications in the GENCL and DIFFR algorithms mounted for nonsingle diffractive and single diffractive interactions, respectively, but only for the Centauro case.

On the other hand, the nature of the produced particles by Centauro and mini-Centauro interactions, whether they are one of ordinary hadrons or particles of some novel nature, emulsion chamber studies have shown that [2, 4] some hadrons among produced secondaries from mini-Centauro interactions make a nuclear interaction in the atmosphere giving rise to a high energy narrow cluster, with a strong penetrative characteristic far beyond the one expected from pure electromagnetic shower developments.

Thus, mini-Centauro events could have triggered the  $Spp\bar{S}$  detectors, but probably they have not a full efficiency to the detection (covering the mini-Centauro  $\eta$  region) of secondary particles produced by mini-Centauro interactions. The expected pseudorapidity distribution according to the DIFFR algorithm (for  $\langle M_X \rangle = 20$  GeV and  $\langle P_T \rangle = 0.38$  GeV/c) and diffractive dissociation such as mini-Centauro events, both to  $\sqrt{s} = 540$  GeV, are shown in Fig. 8.

On the other hand, assuming that around 6% of diffractive events at  $\sqrt{s} = 540$  GeV are mini-Centauro-like events, the experimental data for single-diffractive events, reported by the UA4 collaboration [16], at  $\sqrt{s} = 540$  GeV do not exclude totally a few contributions of mini-Centauro events. The situation is summarized in Fig. 9, where the experimental pseudorapidity distribution of charged particles from the decayed diffractive states with masses of 6–50 GeV is shown, together with predictions of the DIFFR algorithm, and DIFFR+MINICENTAURO algorithms, simulated according to Sec. II is also shown; we can see that the small mini-Centauro contribution is larger just in the region where the experimental pseudorapidity density  $dN/d\eta$  presents a maximum and also is the region where the predictions of the DIFFR algorithm (at  $\langle P_T \rangle = 0.38$  GeV) are not satisfactory (smaller than experimental data).

Centauro and especially mini-Centauro events are expected at Tevatron energies (FERMILAB)  $\sqrt{s} = 1.8$  TeV. However, for the Centauro case the situation is delicate, because the expected energy threshold for Centauro

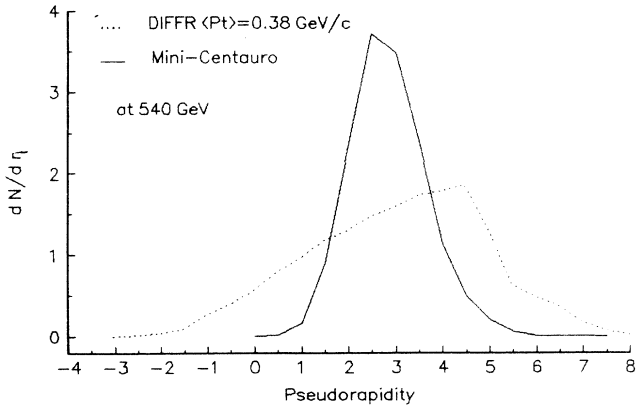


FIG. 8. Pseudorapidity distribution at  $\sqrt{s} = 545$  GeV. The dotted line is according to the DIFFR algorithm with  $M_X = 7 - 50$  GeV and  $\langle P_T \rangle = 0.38$  GeV/c; the solid line is according to the exotic diffractive model for mini-Centauro event production.

events [ $(\sqrt{s})_{th} \sim 2000 \pm 500$  GeV] is consistent with Tevatron energies, while Tevatron energy is big enough for mini-Centauro events.

Reference [17] reports a negative search for Centauro events at the Collider Detector at Fermilab (CDF) in the central rapidity region. This result was expected because the Centauro event is closed with exotic diffractive dissociation. However, in the diffractive region Ref. [18] reports that if the Centauro cross section is truly 4% of the total inelastic cross section, the signal of a diffractively produced Centauro event at CDF would be large and also is described and an adequate trigger sensitive to Centauro events at CDF.

Up to 1991 the status of Centauro and mini-Centauro signals at CDF [19], so far, has not been successful because the CDF detector has noise problems in the forward calorimeter (Texas tower) and also no tracking in the forward region.

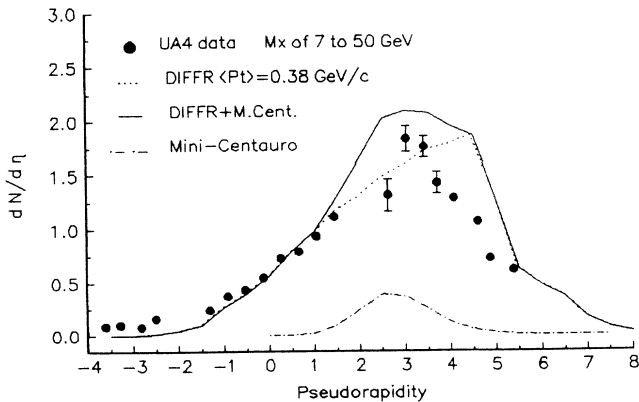


FIG. 9. Pseudorapidity distribution at  $\sqrt{s} = 545$  GeV. The experimental data of diffractive events reported by the UA4 collaboration (solid circles) are compared to a mixture of the DIFFR and EXOTIC diffractive algorithms (solid line), assuming that 6% of diffractive events are like mini-Centauro events.

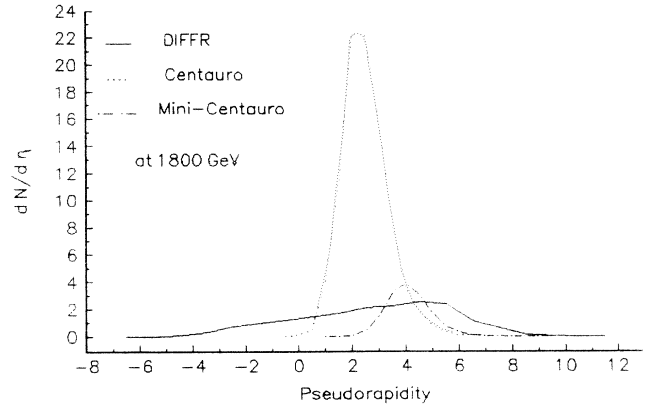


FIG. 10. Pseudorapidity distribution at  $\sqrt{s} = 1.8$  TeV, according to the DIFFR algorithm (solid line), and EXOTIC diffractive algorithm as Centauro (dotted line) and as mini-Centauro (dash-dotted line) events.

A good trigger for diffractive events together with calorimeter and tracking, covering the Centauro and mini-Centauro pseudorapidity regions, can be necessary to discover Centauro and especially mini-Centauro signals at Tevatron energies [20]; in other words, it can confirm or refute the cosmic-ray observations.

The expected pseudorapidity distribution at Tevatron energies ( $\sqrt{s} = 1.8$  TeV), according to the DIFFR algorithm, and diffractive dissociation such as Centauro and mini-Centauro events are shown in Fig. 10. On the other hand, the pseudorapidity distribution, assuming that, at FERMILAB, around 1.52% of diffractive events are Centauro events, 59.2% are mini-Centauro events, and 39% are single “normal” diffractive, is shown in Fig. 11.

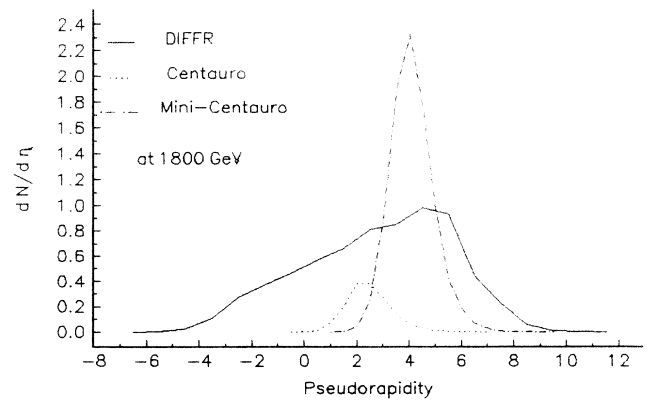


FIG. 11. The same as Fig. 9, assuming that at FNAL 1.5% of diffractive events are Centauro-like, 59% are mini-Centauro-like events and 39% are single “normal” diffractive events.

## V. REEXAMINATION OF CENTAURO PHENOMENA

The negative result of the Centauro search at collider energies (CERN and Fermilab) will lead you to believe that either Centauro events are the result of misunderstanding the experimental observation, or the primary particle of Centauro events is not a proton but some exotic substance such as a quark glob coming from a burst of some quark stars, as suggested by Bjorken and McLerran [21].

On the other hand, it has been suggested also that a Centauro fireball is created in the upper atmosphere by a heavy cosmic-ray nucleus in central collisions with an air nucleus. While, in order for it to survive passage from the upper atmosphere downward to the Chacaltaya altitude, it was proposed that the Centauro fireball has a large mean free path  $\lambda \geq 190 \text{ g/cm}^2$  and/or lifetime around  $10^{-7}$ s [22–24]; thus the hadronization of the Centauro fireball will be near that of the detector.

However, there are a few examples of  $C$  jets (nuclear interaction of hadrons which takes place in the target layer) [2], which are hard to interpret as simple fluctuations of ordinary pion multiple production and the predictions of exotic diffractive dissociation such as mini-Centauro model using  $p\bar{p}$  kinematics are in agreement with these events. Through these events and geometrical considerations of the Chacaltaya chamber, the upper limits to the lifetime and mean free path of mini-Centauro fireballs are estimated as

$$\Delta t < \frac{\Delta y}{c} \sim \frac{0.3 \text{ m}}{c} = 10^{-9} \text{ s}, \quad (13)$$

$$\lambda < \Delta y \sim 60 \text{ g/cm}^2, \quad (14)$$

where  $\Delta y$  is the thickness of the target layer (see Fig. 1). These results strongly support the Centauro species originating in peripheral collisions of hadrons with the nucleus at high energies and also that fireballs such as Centauro species have a lifetime short enough to be essentially irrelevant to the analysis. However, a genetic hypothesis, meaning that the exotic interactions are from exotic particles produced in the exotic interactions of ancestral generation, cannot be discarded.

On the other hand, Ref. [8] has proposed that exotic diffractive fireballs can be the so-called “quark-gluon plasma,” expected in QCD phase transitions, because the temperature increases with fireball mass and its temperature may reach the critical temperature for transition.

Then why does the suppression of  $q\bar{q}$  pairs in the hadronization of exotic fireballs occur? In the last years many authors have suggested several mechanisms to explain the  $q\bar{q}$  suppression; for instance, in Ref. [22] a formation of a “quark-matter fireball” is proposed with large baryochemical potential  $\mu_b$ ; a  $\bar{q}$  is created together with a  $q$  and the large  $\mu_b$  suppresses the production of both. On the other hand, the suppression of  $\pi^0$  in Centauro-like events is explained in Ref. [25] by the formation of pions in the isospin singlet channel; according to this paper, a formation of pions through the  $\sigma$  channel when combined

with symmetrization can lead to a scenario where the isospin distribution is not only broadened but inverted.

## VI. $\gamma$ -RAY FAMILIES AND HADRON INTERACTION CHARACTERISTIC

The cosmic-ray family observation by a high mountain altitude emulsion chamber is a useful tool to study the characteristics of hadron interaction and exotic phenomena which originate from the incidence of extremely high energy cosmic rays into the atmosphere, near around  $10^{16}$  eV or higher, far beyond the reach of present accelerators.

From considerations of the detection efficiency of the shower in the emulsion chamber, the most adequate measurable quantities are the shower energy of electromagnetic origin (“ $\gamma$  rays”), together with the relative position in the chamber. Thus, the total electromagnetic energy  $\sum E_\gamma$  is a good parameter to characterize the “ $\gamma$ -ray” family.

It is well known that the global nature of observed cosmic-ray families is mainly governed by two factors: the chemical composition of the primary cosmic ray and the characteristics of nuclear collision. In order to get knowledge of the global characteristics of hadron interactions at extremely high energies, through family flux observation, experimental results are compared with the results of simulation calculations, under the following assumption.

### A. Primary flux attributes

The primary energy spectrum is assumed as a power type, sampled as

$$I(> E_0) = I_0 \left( \frac{E_0}{1000 \text{ TeV}} \right)^{-\gamma} \quad \text{with } \gamma \sim 1.8, \quad (15)$$

with  $I_0 = 50 \pm 20/\text{m}^2, \text{yr}, \text{str}$ , obtained from air shower experiments [26], where for primary particle composition is observed the so-called “normal” composition, shown in Table V.

### B. Nuclear collision attributes

The code generator which produces the final state particles of the nucleus-nucleus interaction has two parts summarized as follows: Model A = code nucleus + UA5 algorithm; Model B = code nucleus + exotic algorithm.

The first code nucleus, used in both models, described the nucleus-nucleus collision and is a code on the basis of the  $a$  framework, developed by Nihori *et al.* [27]. The nuclear interaction is described by a superposition model, where the nucleus-nucleus collision is divided into a subgroup characterized by values of the number of collisions for intranuclear nucleon-nucleon collisions. A “realistic” treatment of nuclear fragments of the incident nucleus is carried out in order to obtain the number of intranuclear interacting nucleons.

The UA5 algorithm is a code on the basis of GENCL and DIFFR algorithms, reported by the UA5 Group [10] and reproduces nucleon-nucleon collisions ( $\sqrt{s} = 540 - 900$

TABLE V. Assumed composition of primary particles, “normal composition.”

$E$ (eV)	$P$ (%)	$\alpha$ (%)	CNO (%)	Heavy (%)	Very heavy (%)
$10^{15}$	42	17	14	14	13
$10^{16}$	42	13	14	15	16

GeV), for no diffractive and single diffractive interactions, respectively. The basic mechanism of these UA5 Monte Carlo algorithms is the production of hadron clusters and their decay and parameters are chosen so as to reproduce UA5 experimental results as faithfully as possible.

The EXOTIC algorithm is a code that includes exotic channels according to the “exotic diffractive dissociation” picture (see Sec. II this work), under the following statement.

If the incident particle is a baryon, the inelastic nuclear interaction is traced as

$$\text{inelastic interaction} = \text{NSD} + \text{SD} + \text{exotic}, \quad (16)$$

where NSD is a nonsingle diffractive interaction described by the GENCL (UA5) algorithm, SD is a single diffractive interaction described by DIFFR (UA5) algorithm, and exotic is a diffractive production of a baryonic fireball and isotropic decay in baryons, described in Sec. II to report exotic interaction types (Centauro and mini-Centauro).

The branching ratio of exotic-interaction-type production is chosen according to incident energy as follows.

For  $E_N < 100$  TeV,

$$\text{inelastic interaction} = \text{NSD} + \text{SD},$$

$$\text{exotic probability} = 0.$$

For  $100 < E_N < 10^5$  TeV,

$$\text{inelastic interaction} = \text{NSD} + \text{SD} + \text{exotic},$$

$$\text{exotic probability} = 0.333 \ln(E_N/100 \text{ TeV}).$$

For  $E_N > 10^5$  TeV,

$$\text{inelastic interaction} = \text{exotic},$$

$$\text{exotic probability} = 1.$$

If the incident particle is a meson (pion, kaon), we assume

$$\text{inelastic interaction} = \text{NSD} + \text{SD},$$

$$\text{exotic probability} = 0.$$

The situation is summarized in Fig. 2, where the inelastic cross section is drawn as the sum of the cross section of exotic interactions with the cross section of “normal” inelastic processes.

In the code nucleus, the nucleus-nucleus interaction depends strongly on the relative impact parameter between the projectile nucleus of mass  $A$  with a target

nucleus of mass  $B$ ; for instance, if the relative impact parameter is large (peripheral collision), only an inelastic collision between a nucleon of projectile nucleus  $A$  and a nucleon of target nucleus  $B$  is realized; in this case, the nucleus-nucleus interaction is like a nucleon-nucleon, and the number of intranuclear collisions is near 1 ( $N_{\text{coll}} \sim 1$ ). At the other extreme for a small impact parameter (central collision) the number of intranuclear collisions is large [ $N_{\text{coll}} \leq \max(A, B)$ ].

In this work we used the most “realistic” distribution for the number of intranuclear interacting nucleons on the basis of experimental data from both cosmic rays ( $\sim 1$  TeV/nucleon) and machines ( $\sim 200$  GeV/nucleon). According to this scheme, the multiplicity of secondary particles in a nucleus-nucleus interaction is equal to the multiplicity of  $N_{\text{coll}}$  (number of individual nucleon-nucleon collisions), where  $N_{\text{coll}}$  is expressed by

$$N_{\text{coll}} = A - A' - 4N_\alpha - N_{\text{free}} \quad (17)$$

for the process

$$A + B = A' + \text{anything}. \quad (18)$$

Here, the emission of free nucleons  $N_{\text{free}}$  and  $\alpha$  particles  $N_\alpha$  as the most emitted fragment can be explained using thermodynamic considerations [28], where the pre-fragments are treated as a gas, evaporating in free nucleons,  $\alpha$  particles, and others only after an adiabatic expansion. In other words, the final low temperature of the gas favors light fragment formation.

The fragmentation probability of the incoming nucleus  $A$  in  $A'$  (with  $A' > 4$ ) when the target nucleus  $B$  is the air (nitrogen or oxygen) nucleus is taken according to the numerical table summarized by Tsao, Silberberg, and Letaw [29] and for the momentum distribution of a fragment a model with minimal correlation among nucleon moments proposed by Goldhaber [30] is used, where the distribution function that reproduced experimental data is expressed as

$$g(P_f)dP_f = \exp(-P_f^2/2\sigma^2)dP_f/4\pi\sigma^2, \quad (19)$$

with

$$\sigma^2 = \sigma_0^2 A'(A - A')/(A - 1), \quad \sigma_0 = 90 \text{ MeV}/c. \quad (20)$$

The production rate of  $\alpha$  particles  $N_\alpha$  is obtained using a Poisson distribution:

$$P(\langle N_\alpha \rangle, N_\alpha) = 1/N_\alpha!, \quad \langle N_\alpha \rangle^{N_\alpha} e^{-\langle N_\alpha \rangle}, \quad (21)$$

with  $\langle N_\alpha \rangle$  given by the data of Freir and Waddington [31], and for the free nucleon ( $N_{\text{free}}$ ) distribution a function reported by the JACEE Group [32] is used, expressed as

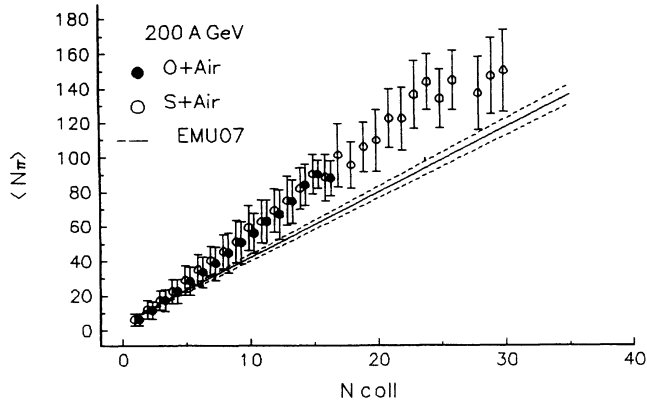


FIG. 12. Correlation between the number of intranuclear collisions  $N_{\text{coll}}$  versus the mean pion multiplicity  $\langle N_{\pi} \rangle$  at 200A GeV, according to model A (solid line) and EMU07 experimental data.

$$f(\chi)d(\chi) = 2\chi d\chi, \quad (22)$$

with

$$\chi = N_{\text{free}} / (A - A' - 4N_{\alpha}). \quad (23)$$

This algorithm used as a model for the nucleus-air nucleus interaction can be considered as a model with a logarithmic time [longer than the (nuclear diameter)/ $c$ ] for secondary particle formation. On the other hand, all these secondary particles have no chance to reinteract inside of the nuclear medium. In this respect the present algorithm is similar to the FRITIOF [33] algorithm that is the Monte Carlo version of the Lund model [34], in contrast with other algorithms, for instance, the HIJET algorithm [35], where the time for secondary particle formation is small and the cascade process in a nuclear medium is considered.

The successful acceleration of oxygen and sulfur ions to 200A GeV at CERN for the several EMU experiments, using emulsion as the target and detector, has shown that superposition hypothesis in nucleus-nucleus collisions is a very good approximation, because a linear correlation between average pion multiplicity with the number of intra nuclear collisions has been found in experimental data [36].

Figure 12 shows the correlation between the average

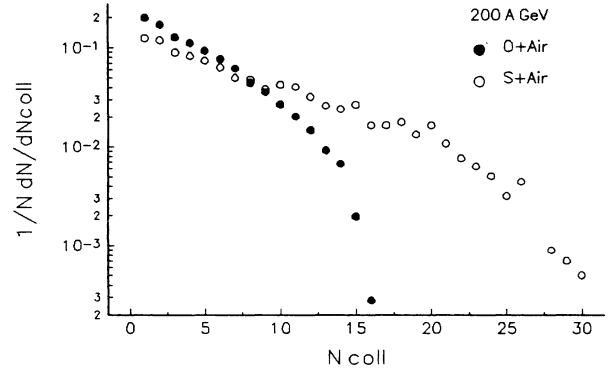


FIG. 13. Distribution of the number of intranuclear collisions  $N_{\text{coll}}$ , in O + air and S + air collisions at 200A GeV, according to model A predictions.

pion multiplicity with the number of intranuclear collisions for the O + air and S + air interaction at 200A GeV according to a prediction of the algorithm used in this work (model A), together with experimental result (EMU07 experiment) reported by the KLM Collaboration [36], for O + emulsion and S + emulsion at 200A GeV plotted as a line and fitted as

$$\langle N_{\pi} \rangle = (3.78 \pm 015)N_{\text{coll}} + (4.14 \pm 0.39). \quad (24)$$

The linear dependence of the mean pion multiplicity over a wide range of the number in intranuclear nucleon-nucleon collisions, irrespective of the mass of the projectile and target, strongly supports the superposition models. The prediction of the present algorithm is in satisfactory agreement with the experimental data; however, for higher values of  $N_{\text{coll}}$  the values of  $\langle N_{\pi} \rangle$  are larger than prediction; this discrepancy can be an effect of any experimental bias not considered in the present algorithm.

It is remarkable that most nucleus-nucleus collisions are nearly peripheral with  $N_{\text{coll}}$  around  $\langle N_{\text{coll}} \rangle$ ; the situation is summarized in Fig. 13 where the predicted  $N_{\text{coll}}$  distributions are plotted for O + air and S + air collisions at 200A GeV. In Fig. 14 we display the pseudorapidity density distribution  $\rho(\eta)$  of secondary particles for O + air and S + air collisions according to the prediction of model A used in this work; it reflects the strong depen-

TABLE VI. Family statistics at Chacaltaya and Pamir, together with observed and expected family flux.

Chamber	Atmospheric depth (g/cm <sup>2</sup> )	Exposure (m <sup>2</sup> ,yr)	No. of families ( $\sum E_{\gamma} > 100 \text{ TeV}$ )	Family flux (m <sup>2</sup> ,yr,str)
Chacaltaya	540	300	121	$0.35 \pm 0.046^{\text{a}}$
Pamir joint	596	530	173	$0.37 \pm 0.032$
Pamir (a part)	596	400	135	$0.30 \pm 0.033$
model A	596	(include UA5 algorithm)		$1.48 \pm 0.6$
model B	596	(include UA5 and EXOTIC algorithms)		$0.26 \pm 0.033$

<sup>a</sup>Expected at Pamir by assuming  $\lambda_{\text{att}} = 100 \text{ g/cm}^2$ .

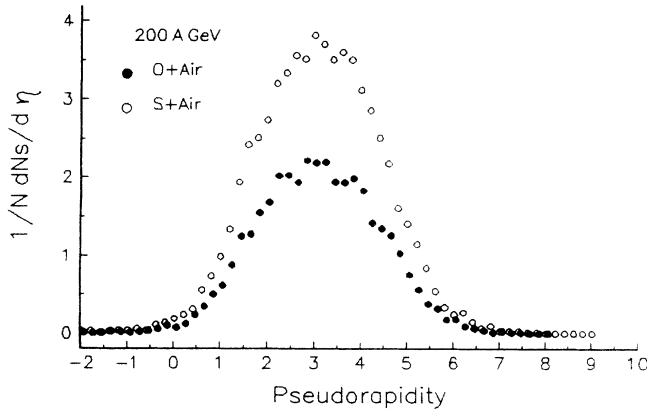


FIG. 14. Pseudorapidity distribution of the produced charged secondaries in O + air and S + air collisions at 200 A GeV, according to model A predictions.

dence of  $\rho_{\max}$  with an ion projectile mass.

On the other hand, the observed families represent the hadron interactions after a few generations of successive atmospheric interactions. The main contribution to the  $\gamma$ -ray family particles ( $\gamma, e^{\pm}$ ) comes from  $\pi^0 \rightarrow 2\gamma$  decay; thus, the  $\gamma$ -ray propagation through the atmosphere is traced via Monte Carlo methods using the conventional electromagnetic cascade theory.

Table VI summarizes the statistics of “ $\gamma$ -ray” families, with a visible energy greater than 100 TeV, under the detection threshold  $E_{\text{th}} = 4$  TeV, observed in three independent experiments: Chacaltaya Chamber, Pamir-Chacaltaya joint Chamber, and Pamir Chamber; the observed and predicted (according to models A and B) values of the “ $\gamma$ -ray” family flux are also shown.

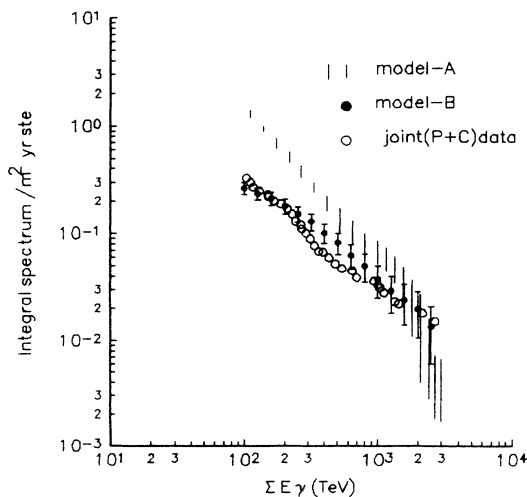


FIG. 15. Integral spectra of  $\gamma$ -ray energy sum of a family,  $\sum E_{\gamma}$ . The open circles represent 175 families in the Pamir-Joint Chamber at Pamir, and are compared with results from simulation calculations, according to model A (vertical lines) and model B (solid circles), both under the assumption of a normal chemical composition in the primary flux.

Figure 15 shows the integral spectrum of the family energy in the form of an energy sum of “ $\gamma$  rays,”  $\sum E_{\gamma}$ ; the open circles represent the 175 families in the Chacaltaya Pamir “joint Chamber” at Pamir, while the vertical lines and solid circles represent the energy spectra for families obtained by simulation calculations according to models A and B, respectively. The agreement between model B with experimental data is satisfactory. However, the spectrum according to model A is larger than experimental data, especially in the lower energy region.

## VII. CONCLUSIONS

The successful prediction of exotic diffractive dissociation, as the production of energy threshold (in agreement with experimental data and other models), as well as the pseudorapidity distribution and midrapidity and others, for both Centauro and mini-Centauro events, strongly supports that Centauro-like events are a result of isotropic decay of exotic fireballs produced coherently in diffractive dissociation; from this picture we can also see that Centauro-like events are close to kinematics of nucleon-nucleon collisions, and this supports that both Centauro and mini-Centauro events originate in peripheral proton-nucleus or nucleus-nucleus collisions.

The peculiarities of exotic characteristics are observed in the forward region, where cosmic-ray observation presents a whole potential, while collider experiments suffer observational restrictions. However, the diffractive experimental data at  $Spp\bar{p}S$  does not totally exclude a few contributions of mini-Centauro-like events.

Emulsion chamber experiments at mountain altitudes have shown that the “ $\gamma$ -ray” family flux is much lower than simulated results based in the so-called “ln s” extrapolation of models on the basis of accelerator data, for instance, the UA5 algorithm. Thus, the effect of including exotic processes in nuclear interactions of cosmic-ray particles with atmospheric nuclei reduces the expected electromagnetic family flux, because the production of  $\pi^0$ 's (consequently “ $\gamma$  rays”) in Centauro-like events is suppressed by some understood mechanism. Of course, the energy dependence of the cross section to exotic process is assumed crude here, especially in the extremely high energy region, and is chosen so as to reproduce “ $\gamma$ -ray” family results as faithfully as possible, while it is in agreement with the prediction of exotic diffractive dissociation in the lower energy region as the threshold energy for Centauro-like event production.

On the other hand, from the analysis of family flux, we can see that the frequency of Centauro-like events is not small, and appears in a global structure of family analysis and reflects the characteristic behavior of particle production at the parent interaction.

We are waiting for the new diffractive results at Fermilab as well as from the next Large Hadron Collider (LHC) at CERN to confirm or to disprove the existence of such exotic interactions or, at least, to make clear if they are a product of nuclear collisions or are celestially born.

## ACKNOWLEDGMENTS

The authors are most grateful to all the colleagues of the Chacaltaya Collaboration, without whose continuous contribution the present work could not have been

completed. We especially thank Professor M. Tamada for his suggestions and valuable computational software support. This work was partially supported by FINEP and FAPESP (Brazilian Government Agencies).

- 
- [1] C.M.G. Lattes, Y. Fujimoto, and S. Hasegawa, *Phys. Rep.* **65**, 151 (1980).
- [2] S. Hasegawa, ICR Report No. 151-87-5, Tokyo, 1987 (unpublished).
- [3] M. Tamada, in *Proceedings of the 23rd International Cosmic Ray Conference*, Calgary, Canada, 1993, edited by D. A. Leahy (University of Calgary, Calgary, 1993), Vol. 6, p. 13.
- [4] Chacaltaya and Pamir Collaborations, *Nucl. Phys.* **B370**, 365 (1992).
- [5] A. Ohsawa and K. Sawayanagi, *Phys. Rev. D* **45**, 3138 (1992).
- [6] A.M. Dunaevsky and N.P. Krutikova, in *Proceedings of the VIIth International Symposium on Very High Cosmic Ray Interactions*, Ann Arbor, MI, 1992, edited by L. W. Jones, AIP Conf. Proc. No. 276 (AIP, New York, 1993), p. 540.
- [7] K. Goulianos, in *Proceedings of the W.P.S.H.E.*, University of Wisconsin-Madison, edited by V. Barger, W. H. Gottschalk, and F. Halzen (World Scientific, Singapore, 1986), p. 299.
- [8] K. Goulianos, *Comments Nucl. Part. Phys.* **17**, 195 (1987).
- [9] M. Tamada, in "Proceedings of the International Workshop on Super High Energy Hadron Interaction," report, Tokyo, 1991 (unpublished), p. 263.
- [10] UA5 Collaboration, *Nucl. Phys.* **B258**, 505 (1987).
- [11] UA5 Collaboration, CERN Report No. EP/86-127, 1986 (unpublished).
- [12] K. Kang and A. White, *Phys. Rev. D* **42**, 835 (1990).
- [13] T.H. Burnet *et al.*, *Astrophys. J.* **349**, 25 (1990).
- [14] M. Ichimura *et al.*, *Phys. Rev. D* **48**, 1949 (1993).
- [15] A.M. Hillas, in *Proceedings of the 16th International Cosmic Ray Conference*, Kyoto, Japan, 1979, edited by S. Miyake (University of Tokyo, Tokyo, 1979), Vol. 6, p. 13.
- [16] UA4 Collaboration, *Phys. Lett.* **166B**, 459 (1986).
- [17] D. Amidei, *CDF/ANAL/MINBIAS/CDFR/672*.
- [18] D. Amidei, *CDF/MEMO/MINBIAS/CDFR/672*.
- [19] Y. Funayama (private communication).
- [20] K. Goulianos, in *Proceedings of the VIIth International Symposium on Very High Cosmic Ray Interactions* [6], p. 244.
- [21] J.D. Bjorken and L.D. Mclerran, *Phys. Rev. D* **20**, 2353 (1979).
- [22] A.D. Panagiotou, A. Petridis, and M. Vassiliou, *Phys. Rev. D* **35**, 3134 (1992).
- [23] S. Errede, *CDF/ANAL/CDF/CDFR/690*.
- [24] P.B. Price, *Phys. Rev. D* **47**, 5194 (1993).
- [25] S. Pratt and V. Zelevinsky, *Phys. Rev. Lett.* **72**, 816 (1994).
- [26] S.I. Nikolsky, in "Proceedings of the International Symposium on Cosmic Rays and Particle Physics," report, Tokyo, 1984 (unpublished), p. 507.
- [27] Y. Niihori, T. Shibata, I. Martin, E. Shibuya, and A. Turtelli, *Phys. Rev. D* **36**, 783 (1987).
- [28] A. Freidman and W.G. Lynch, *Phys. Rev. C* **28**, 16 (1983).
- [29] C.H. Tsao, R. Silberberg, and J.R. Letaw, in *Proceedings of the 18th International Cosmic Ray Conference*, Bangalore, India, 1983, edited by N. Durgaprasad (TIFR, Bombay, 1983), Vol. 2, p. 294.
- [30] A.S. Goldhaber, *Phys. Lett.* **53B**, 306 (1974).
- [31] P.S. Freier and C.J. Waddington, *Astrophys. Space Sci.* **38**, 419 (1975).
- [32] JACEE Collaboration, in *Proceedings of the IV International Conference on Ultra-relativistic Nucleu-Nucleus Collisions*, Helsinki, Finland, 1984, edited by K. Kajantie (Springer, New York, 1985).
- [33] B. Nilsson-Almqvist and E. Stenlund, *Comput. Phys. Commun.* **43**, 374 (1987).
- [34] B. Anderson, G. Gustafson, and B. Nilsson-Almqvist, *Nucl. Phys.* **B178**, 242 (1981).
- [35] T.W. Ludlam, BNL Report No. 97, 1983 (unpublished); BNL Report No. 31, 1983 (unpublished).
- [36] KLM Collaboration (EMU07 experiment), *Phys. Rev. D* **47**, 1751 (1993).

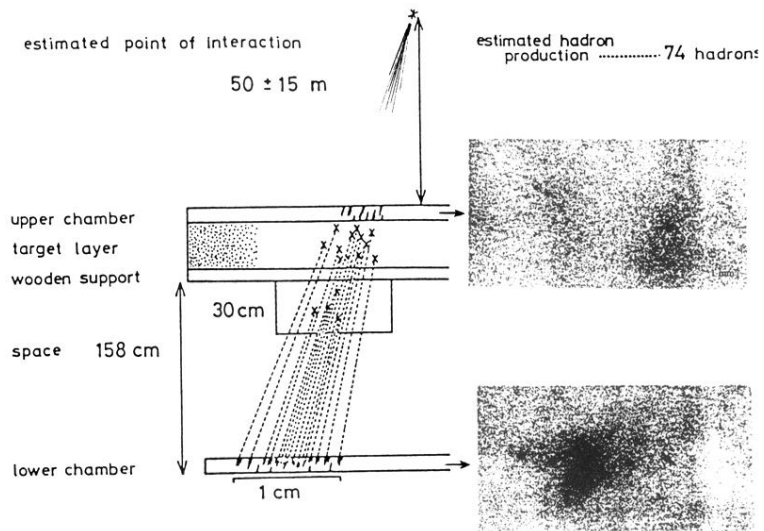


FIG. 1. Schematic view of structure of Chacaltaya two-story chamber, together with photographs of Centauro I as viewed in x-ray films of the upper and lower chambers.